Characterization of Size-Exclusion Effects in Highly Swollen Hydrogels: Correlation and Prediction

ALEXANDER P. SASSI, HARVEY W. BLANCH, and JOHN M. PRAUSNITZ*

Chemical Engineering Department, University of California, Berkeley, California 94720 and Chemical Sciences Division, Lawrence Berkeley Laboratory, Berkeley, California 94720

SYNOPSIS

The literature provides several size-exclusion theories to predict solute exclusion by highly swollen hydrogels. Theoretical calculations are compared to the experimental data of Walther et al. (1993) for partitioning of poly(ethylene glycol)s and poly(ethylene oxide)s of various molecular weight into hydrogels made of poly-*N*-isopropylacrylamide or poly-2-hydroxyethyl methacrylate/dimethylaminoethyl methacrylate. Experimental size-exclusion curves can be correlated almost equally well by theories which characterize the gel as a collection of pores or of fibers; differences between these two theories are important only for partition coefficients near zero or unity. The experimental data of Walther et al. can be predicted best by Schnitzer's uniform pore model. © 1996 John Wiley & Sons, Inc.

INTRODUCTION

The distribution of solutes between a gel and its surroundings is important in several applications of gels. For example, the effective separation of a mixture of solutes by liquid column chromatography depends on the relative equilibrium distribution (partitioning) of the different solutes between the chromatographic packing and the solution flowing through the column. The equilibrium distribution of a solute between a gel and its surroundings is characterized by the solute partition coefficient, which we define as the ratio of the concentration of the solute in the gel to that in the gel's surroundings.

Solute distribution into a swollen polymer network (gel) depends on the interactions of the solute with the polymer network. The simplest realistic interaction between a solute and a polymer network is steric exclusion; the solute may not occupy any space simultaneously occupied by the polymer. For simple size exclusion, the potential of mean force between a solute and the polymer is infinite for solute–polymer separations smaller than the distance of closest approach (defined solely by the geometry of the solute and polymer) and zero for solute–polymer separations greater than the distance of closest approach. Considerable theoretical effort has been expended to describe the steric or size exclusion of solutes by porous media; the main difficulty lies in properly characterizing a medium where the geometry is unknown. Therefore, the medium is usually modeled as a collection of volume elements of uniform geometry.

To predict theoretically the complex situation where there may be attraction between gel and solute, we must first be able to predict, or at least correlate, steric exclusion. To assure that we have predicted size exclusion successfully, we must compare calculated results to experimental partitioning data taken for a solute which experiences only steric interactions with the network. In principle, this is possible, but as Hussain et al. discussed, such an ideal solute may not exist.[1] Thus, we compare calculations to experimental data for those systems where we hope to have minimized other interactions. We evaluate how well existing models predict and correlate size-exclusion phenomena so that we may use these models, in part, toward prediction of partitioning in more complicated systems.

We begin by comparing the partition coefficients predicted by several size-exclusion models. We examine the qualitative dependence of the partition

* To whom correspondence should be addressed.

Journal of Applied Polymer Science, Vol. 59, 1337–1346 (1996)
 CCC 0021-8995/96/081337-10

coefficient on solute size and on nominal gel-composition parameters. Hussain et al.[1] presented an excellent comparison of how size-exclusion models can be used to correlate experimental partitioning of polymers in porous glass or Sephadex, which are not highly swollen. Hussain et al. concluded that the best way to correlate experimental data is to use a size-exclusion model which accounts for a pore-size distribution; this distribution, however, must be determined experimentally. For gels, it is difficult to obtain pore-size distribution data; therefore, such data are scarce.

In the size-exclusion-chromatography literature, two descriptions are used for the morphology of the porous medium (the hydrogel). In the fiber model, the swollen polymer network is a meshwork of cylindrical fibers. The morphology of the matrix is characterized by dimensions of the fibers themselves.

In the pore model, the swollen polymer network is a solid phase containing a number of pores of some defined geometry (planes, spheres, or cylinders). The morphology of the matrix is characterized by some measure of the mean size of the pore and sometimes also by the distribution of pore sizes. The pore and fiber models are basically equivalent but inversely related in perspective; one attempts to characterize the volume occupied by the fibers, and the other attempts to characterize the volume not occupied by the fibers.

For hydrogels, the concept of a pore-size distribution is ambiguous because we do not expect the space between polymer strands to be simple, uniform tubes. The pore-size distribution of a hydrogel cannot be easily determined, except perhaps through data from solute partitioning experiments—the very type of data one hopes to predict. In the absence of suitable partitioning data, the pore size of a gel may be estimated by half the corresponding mesh size of a solution of uncrosslinked polymer,[2] which returns us to the perspective of the fiber model. Predictions of fiber and pore models should agree to a large extent. We now examine whether this is indeed the case.

THEORETICAL CALCULATIONS

Models for Size Exclusion

From the work of Ogston,[3] Laurent and Killander[4] developed the following expression (the LKF model) for the partitioning of a spherical solute of radius r_s into a solution of randomly arranged rigid rods of radius r_f:

$$K = \exp[-\pi L(r_f + r_s)^2] \quad (1)$$

where K is the partition coefficient of the solute (here equal to the fraction of the gel volume accessible to the solute) and L is the length of the fibers per unit volume.†

Schnitzer also derived general expressions for the volume fraction accessible to a solute particle.[5] For uniform distributions of volume elements, where in each subunit volume the polymer chains can only adopt a single conformation, the expressions derived by Schnitzer agree with those of Ogston, who treated spherical solutes,[3] and those of Giddings et al., who considered nonspherical geometry.[6] Yasuda et al.[7] and Peppas and Reinhart[8] also investigated the volume fraction accessible to a rigid solute; however, their work concerns solute permeation through membranes.

For random distributions of volume elements, where in each subunit volume the polymers can adopt many conformations, Schnitzer's expressions agree with those of Giddings et al. in the limit of a low polymer volume fraction and infinitely small solutes. Schnitzer's expressions are able to correlate quantitatively data in electrophoresis and size-exclusion chromatography.[5] For the distribution of a spherical solute in a randomly oriented and distributed meshwork of cylindrical fibers, neglecting fiber-end effects, Schnitzer developed the following expression (the SRF model):

$$K = \exp(-\nu_e^0)\exp\{\nu_e^0[1 - (1 + r_s/r_f)^2]/(1 - \nu_e^0)\} \quad (2)$$

where ν_e^0 is the volume fraction of the gel excluded to a point solute. The volume fraction of the gel excluded to a point solute may be estimated by the volume fraction of the polymer in the gel phase (ϕ_p). The solute radius is taken to be the hydrodynamic radius (R_{hyd}) obtained from the Stokes–Einstein equation:

$$r_s = R_{hyd} = (k_b T)/(6\pi D_0 \eta_0) \quad (3)$$

where k_b is the Boltzmann constant; η_0, the viscosity of the solvent; D_0, the diffusion coefficient of the solute at infinite dilution; and T, the temperature. The fiber radius can be estimated by electron microscopy or, in the absence of such data, by assuming that the radius of the fiber is approximately the

† The length of fibers per unit volume is given by $L = (1/V)\sum_i n_i L_i$, where L_i is the length of an individual fiber and n_i is the number of fibers in volume V.

length of the longest repeated pendant group on the polymer backbone.‡

For the volume exclusion of spherical solutes in cylindrical pores, Schnitzer derived the following expressions[5]:
For uniformly distributed pores (the SUP model):

$$K = \nu_c^0(1 - \beta)^2 \tag{4}$$

for randomly distributed pores (the SRP model):

$$K = \exp(\nu_c^0 - 1)\exp(\beta^2 - 2\beta) \tag{5}$$

where β is the ratio of solute to pore radius, r_s/r_p, and ν_c^0 is the volume of pore space per unit volume (the porosity).

Universal calibration curves in size-exclusion gel chromatography are often constructed using partitioning data for polymeric solutes. The conformation of a polymer in solution fluctuates about some equilibrium average, and the average volume in which the polymer chain resides, but does not necessarily fill, is often described as a sphere of given radius. Because the polymer can adopt different configurations, it is possible for a polymer whose average occupied space is characterized by a radius r to penetrate a given matrix to a greater extent than a rigid sphere of the same radius r. An example is provided by the well-known reptation mode of polymer diffusion, whereby the polymer moves through a matrix of obstacles much as a snake through a dense sugarcane field. Clearly, if the snake were to adopt a spherical conformation and try to roll into the center of the field (where the mean spacing between canes is on the order of the radius of the balled-up snake), it would not be able to move through as much of the field as if the snake were to slither normally. Casassa was the first to consider this effect for random-flight chains penetrating pores of simple geometry.[9] For cylindrical pores, Casassa found the following expression, valid for the limiting case of a chain of an infinite number of vanishingly small segments:

$$K_{\text{chain}} = 4 \sum_{n=1}^{\infty} B_n^{-2} \exp[B_n^{-2}(\langle s^2\rangle/r_p^2)] \tag{6}$$

$$J_0(B) = 0 \tag{7}$$

where J_0 denotes the Bessel function of the first kind of order zero and $\langle s^2\rangle$ is the mean square radius of gyration for the chain solute.[9-11,§]

Davidson et al. performed Monte Carlo simulations to expand the work of Casassa to account for finite numbers of chain segments of finite length.[12] They approximated the Monte Carlo results with the following expression (the DP model):

$$K = \ln(K_{\text{Casassa}}) + (1/r_p)(0.49 + 1.09\lambda_G + 1.79\lambda_G^2) \tag{8}$$

$$\lambda_G = \sqrt{\langle s^2\rangle}/r_p \tag{9}$$

where 1 is the step length of the polymer chain.

‡ Here, we assume that the spatial distribution of pendant groups around the polymer backbone describes a cylinder whose axis is the polymer backbone. The radius of this cylinder is the length of the pendant group.

§ Casassa's partition coefficient is not the same as ours. Casassa's partition coefficient is the ratio of the concentration of a solute inside the pores of the matrix to that outside the matrix and therefore does not take into account the volume of the matrix. This can be seen by comparing the values of the partition coefficient for infinitely small solutes. By our definition, the partition coefficient of an infinitely small solute would be equal to $1 - \nu_e^0$ ($= 1 - \phi_p$). Casassa's results show a partition coefficient of 1 for infinitely small solutes. Therefore, to compare properly Casassa's predictions to experimental data, we must multiply Casassa's partition coefficient by the factor $(1 - \phi_p)$ to obtain the correct limiting behavior.

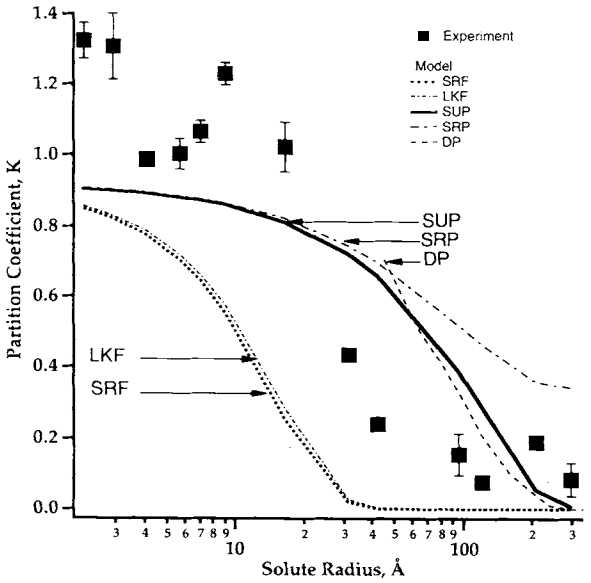

Figure 1 Effect of solute radius on partition coefficient for partitioning of PEG and PEO into poly-NIPA hydrogels (15%T, 1%C) in water at 25°C. Experimental data are shown by filled squares. Calculated partition coefficients using five models for size exclusion are also presented (lines). A fiber radius of 5.5 Å was used in all fiber-model calculations, and a pore radius of 262 Å was used in all pore-model calculations. Calculated partition coefficients are predictions.

Prediction of Size Exclusion

In Figure 1, we compare partition coefficients for solutes of differing radius calculated using the models discussed above. The matrix is a poly(*N*-isopropylacrylamide) (poly-NIPA) hydrogel (15%*T*, 1%*C*) in 0.001*M* NaN_3 (as an antibacterial) at 25°C where the parameters %*T* and %*C* are defined by

%*C*: mol % crosslinking monomer,

%*T*: g of total monomer/100 mL water at synthesis.

The volume fraction of this hydrogel is approximately 0.07, based on the swelling capacity reported by Walther et al.[13] Because swelling of poly-NIPA hydrogels is extremely sensitive to temperature at ambient and near-ambient conditions, size-dependent solute separation and concentration schemes have been proposed which take advantage of the unique swelling behavior of poly-NIPA gels. We therefore desire to predict the partition coefficients for solutes into poly-NIPA gels. Walther et al. measured the distribution of poly(ethylene glycol)s (PEG) and poly(ethylene oxide)s (PEO) between the external solution and poly-NIPA gels; his data are also presented in Figure 1 for comparison.[13] We do not expect the calculated partition coefficients to agree with the experimental data of Walther et al., because these data clearly illustrate that size exclusion is not the only mechanism governing the solute distribution. We merely wish to compare the qualitative behavior of predictions where model parameters are *not* obtained from partitioning experiments. Based on this comparison, we select the simplest, qualitatively correct model and attempt to represent size-exclusion effects by adjusting one of the model parameters, such as the fiber or pore radius. This adjustment allows us to progress later to the more interesting and difficult task of predicting partition coefficients of proteins in charged hydrogels.

We now briefly discuss how the parameters for each model were obtained for the 15%*T*, 1%*C* poly-NIPA gel at 25°C. For the fiber-matrix models [LKF model, eq. (1), and SRF model, eq. (2)], the fiber radius was obtained by using standard bond lengths and angles to calculate the length of the groups extending from the carbon backbone of the polymer. For poly-NIPA, the fiber radius was calculated to be approximately 5.5 Å. This calculation presupposes that individual polymer strands are not bundled together. In the LKF model [eq. (1)], the fiber length density (L) was then calculated from the polymer volume fraction (ϕ_p) and the fiber radius (r_f). In the SRF model, the fractional volume inaccessible to a point solute (v_e^0) was taken to be the polymer volume fraction (ϕ_p).

The mean pore radius [needed for eqs. (4)–(9)] was determined as one-half the mesh size (ξ) calculated by following the methods of Peppas et al.[2] The mesh size of a polymer matrix is related to the volume fraction of polymer and the mean end-to-end distance of the chains of the network as defined by the crosslink density:

$$\xi = \phi_p^{-1/3}\langle r_{e-e}^2\rangle^{1/2} \tag{10}$$

where $\langle r_{e-e}^2\rangle$ is the mean square end-to-end distance. The mean square end-to-end distance for a random-flight chain is related to the mean square radius of gyration:

$$\langle r_{e-e}^2\rangle = 6\langle s^2\rangle \tag{11}$$

Kubota et al. measured (via light scattering) the radii of gyration for linear poly-NIPA in water as a function of molecular weight and temperature.[14] To estimate the average molecular weight between crosslinks, $\bar{M}_c$, the nominal %*C* was used:

$$\bar{M}_{c,\text{nominal}} = 0.5(\text{MW}_{\text{monomer}}/X) \tag{12}$$

$$X = \%C/(100 - \%C) \tag{13}$$

where $\text{MW}_{\text{monomer}}$ is the molecular weight of the monomer. The average molecular weight between crosslinks was determined to be 5600 g/mol. The shortest poly-NIPA studied by Kubota et al. had a molecular weight of 1.63×10^6 g/mol and a radius of gyration ($\langle s^2\rangle^{1/2}$) at 20°C of 510 Å. Using the following scaling method, the radius of gyration for poly-NIPA of molecular weight 5600 g/mol was estimated to be approximately 95.3 Å:

$$\langle s^2\rangle^{1/2} \propto N^{1/3}\tau^{-1/3} \tag{14}$$

$$\tau = \frac{T - \theta}{\theta} \tag{15}$$

where θ is the theta temperature, here defined as that temperature where the second osmotic virial coefficient for the polymer becomes zero (30.6°C for poly-NIPA) and N is the number of monomers of the chain (the degree of polymerization). For this value of the radius of gyration, the pore radius was 262 Å. The DP model [eqs. (8)–(9);[12]] also requires the length of a segment of the polymer chain, which

we took to be 2.52 Å, the approximate distance between alternate carbons on the backbone.

The partition coefficients calculated using the LKF and SRF models are virtually identical, which we expect because the volume fraction of polymer is low. The shape of the size-exclusion curve (the curve defined by the relation between partition coefficient and solute radius) is sigmoidal, as obtained from experiment. The size-exclusion curves obtained using the SUP and SRP models are sinusoidal, as are those for the fiber matrix (LKF and SRF) models, but the region where the partition coefficient is most sensitive to solute radius appears broader. This region is of primary importance for applications where gels are used to separate solutes of different sizes. The SRP model incorrectly predicts that, in the limit of equal solute and pore radii, the partition coefficient approaches $\exp(-1 - \nu_e^0)$. Therefore, we do not consider further the random-pore (SRP) model. The DP model predicts slightly lower partition coefficients when $r_s/r_p \geq 0.5$ as compared to the SUP model but has the more correct limiting behavior for polymer chains, viz., partition coefficients are not zero for $\langle s^2 \rangle^{1/2}/r_p \geq 1$. The corrections of Davidson et al. become significant when the segment size approaches the pore radius; for relatively highly swollen gels (such as the poly-NIPA gel considered here), the corrections of Davidson et al. are not significant. A closer examination of the general shapes of the size-exclusion curves predicted by the fiber (LKF and SRF) and uniform cylindrical-pore models (SUP) reveals that the experimental data are (surprisingly) well bounded by the two models; the pore model represents the data for small solute radii better, while the fiber model is better for larger solute radii. We emphasize that the calculations require no data from partitioning experiments.

Size-exclusion curves depend on the volume excluded by the matrix. For a hydrogel, the volume of the matrix at equilibrium in excess water depends on gel composition and on synthesis and solution conditions. Walther et al. also reported data for the same gel and solutes at 32°C, where the volume fraction of the polymer is approximately 0.15, twice that at 25°C.[13] For a solute of a given radius, the ratio of the partition coefficient at 32°C to that at 25°C was calculated using the SUP and SRF models. Figure 2 compares calculated results to experimental data. The fiber model (SRF) predicts a much more significant decrease in partitioning with the temperature increase as compared to the pore model (SUP). For solute radii less than 30 Å, the SUP model represents the effect of temperature fairly well. Freitas reported partitioning data for PEG 3400

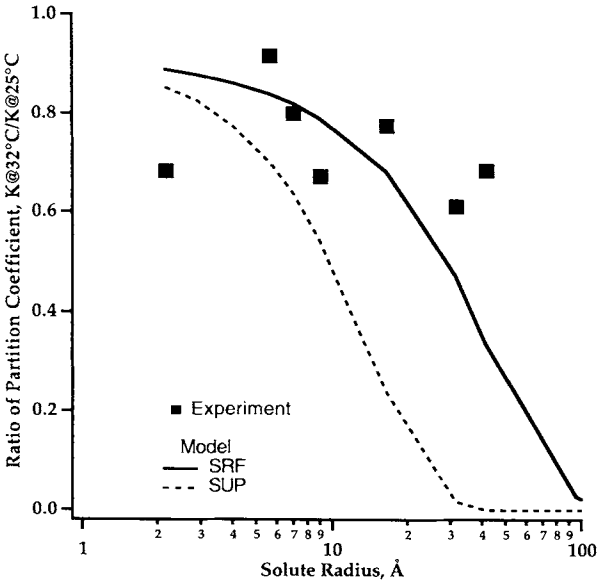

Figure 2 Effect of temperature and solute radius on partitioning of PEG and PEO into poly-NIPA hydrogels (15%T, 1%C) in water at 25° and 32°C. Experimental data are shown by filled squares. Calculated results are shown by lines. Calculated results show that the partition coefficient declines as temperature increases. The partition coefficier t declines more for large solutes than for small solutes. The experimental data do not exhibit the same pattern of decrease in the partition coefficient as that shown by the calculated results.

in poly-NIPA gels of varying %C (8%T).[15] For these data, the calculations based on the SRF model lie much closer to the experimental data than do those based on the SUP model (Fig. 3). Freitas also reported partitioning data for PEG 3400 in poly-NIPA gels of varying %T (1%C), but the dependence of the swelling capacity on %T obtained from his experimental data is not monotonic, contrary to our experience. Therefore, we did not evaluate the size-exclusion models for varying-%T poly-NIPA hydrogels.[15]

The effects of %T or %C are taken into account differently in the pore (SUP, SRP, and DP) and fiber models (LKF and SRF). In the fiber model, the effect of %T or %C appears only in the parameter ν_e^0, which is simply a measure of the water content of the swollen gel. In the calculations performed above, the effect of %C in the pore model is taken into account in both parameter ν_e^0 *and* the pore radius (via the calculation of the molecular weight between crosslinks using the *nominal* crosslink density). The effect of %T in the pore model in the calculations above is *not* taken into account via the pore radius. However, we do not expect the true crosslinking of

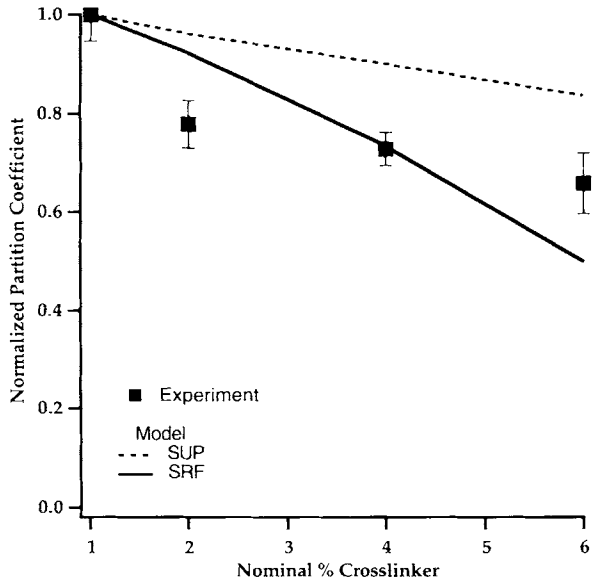

Figure 3 Effect of $\%C$ on the partition coefficient for PEG 3400 in poly-NIPA gels in water. The partition coefficient was normalized to that for the gel with $1\%C$ to determine whether Schnitzer's pore and fiber models could correctly account for the effect of increasing $\%C$. The calculated results using the fiber model (solid line) agree best with the experimental data (squares). Experimental data from Freitas.[15]

the gel to be the nominal $\%C$. This expectation is confirmed by swelling equilibria which show significant effects of $\%T$; theoretical calculations cannot describe quantitatively the effects of $\%T$.[16,17] If we could calculate the effective topographical crosslink density at various $\%T$ and $\%C$, we might then be better able to calculate the relative effects of changing $\%C$ and $\%T$ on size-exclusion curves. We realize that effective crosslink densities depend on their method of determination; previous work has indicated that crosslink densities based on stress–strain measurements differ from those based on swelling measurements.[18] Unfortunately, there are not sufficient data in the literature to predict confidently effective crosslink densities for poly-NIPA hydrogels.

Therefore, to examine better the effects of $\%T$ and $\%C$, we considered hydrogels of 2-hydroxyethyl methacrylate (HEMA), because sufficient data exist to estimate effective crosslink densities.[2,19–21] Unlike poly-NIPA hydrogels, poly-HEMA gels are not temperature-sensitive. Walther et al. also reported data for partitioning of PEG and PEO into cationic poly-HEMA/dimethylaminoethyl methacrylate (DMA) hydrogels of varying $\%C$ and $\%T$ in aqueous NaN_3.[22] The molecular weight between effective crosslinks was calculated using information from swelling equilibria for the cationic gels and from stress–strain measurements on neutral poly-HEMA gels. The molecular weight between effective crosslinks was smaller than that calculated using the nominal value of $\%C$, so much so that the size-exclusion curves predicted using an effective crosslink density were much farther removed from the experimental data than either the calculations with the SRF model or the SUP model using the nominal $\%C$. The effective crosslink density did not help in predicting the effect of $\%C$ on the size-exclusion curves. Thus, we conclude that for the cationic poly-HEMA/DMA gels calculation of an effective crosslink density is an unnecessary effort. For neutral gels, this approach may be of some use, but we did not have appropriate data to pursue that approach.

The models were derived for solutions infinitely dilute in solute, and, therefore, the calculated partition coefficient does not depend on solute concentration. Fanti and Glandt investigated the concentration dependence of solute partitioning with density functional theory and Monte Carlo simulation.[23,24] We used their Monte Carlo results for partitioning of hard spheres into a fibrous matrix to determine whether concentration effects were important for the range of polymer concentrations used by Walther et al. The correction for the effect of solute concentration was negligible.

Correlation of Size-Exclusion Data

From the observations in the previous section, we chose to fit experimental partitioning data for PEG and PEO in poly-NIPA and poly-HEMA/DMA hydrogels using the SRF and SUP models. Only one parameter was adjusted in each model: r_f for the fiber model and r_p for the pore model. We minimized the sum of the squared residuals between calculated and experimental values reported by Walther et al. The resulting best-fit radii are compared in Table I with the a priori-calculated radii and the mean pore radii determined by Walther et al. using the model of Casassa.[9] Figure 4 presents a comparison of size-exclusion curves calculated with fit and predicted (nonfit) parameters with experimental data for PEG and PEO partitioning in poly-NIPA hydrogels at 32°C ($15\%T$, $1\%C$). The difference between size-exclusion curves using the fit (21 Å) and calculated (5.5 Å) values of the fiber radius (SRF model) is much greater than that between the corresponding curves for the SUP model (fit pore radius: 84 Å; calculated pore radius: 111 Å). Nevertheless, when used to correlate experimental data, both SRF and

Table I Comparison of Fit and Predicted Parameters for Size-Exclusion Models

Gel: poly-NIPA, 15%*T*, 1%*C*

Parameter (Å)	25°C	32°C
Pore radius (Walther, 1993)	54.2	28.5
Pore radius, fit	163	84
Pore radius, predicted	262	111
Fiber radius, fit	21	21
Fiber radius, predicted	5.5	5.5

Gel: poly-HEMA/DMA, 65%*T*, various %*C* and %DMA, 25°C

Parameter (Å)	Gel*					
	1	2	3	4	5	6
Pore radius (Walther et al.[13])	68	138	74	74	62	66
Pore radius, fit	161	207	138	136	123	130
Pore radius, predicted	108	136	108	125	55	58
Fiber radius, fit	21	17	19	11	14	14
Fiber radius, predicted	6.3	6.3	6.3	6.3	6.3	6.3

* Gel	%*C*	%DMA	Polymer volume fraction
1	0.2	10	0.073
2	0.2	10	0.037
3	0.2	7	0.075
4	0.2	7	0.047
5	0.2	10	0.069
6	0.2	10	0.058

SUP models predict virtually the same size exclusion curve, as expected. This agreement implies that we can use either model, adjusting only one parameter, to *correlate* experimental size-exclusion data. If we wish to *predict* the size-exclusion curve for a material where the pore-size distribution is unknown, we can use the uniform cylindrical pore model (SUP) provided that the end-to-end distance of the uncrosslinked polymer chains (of which the network is synthesized) is available experimentally from data such as light scattering. Figure 5 presents similar data as in Figure 4 but for a poly-HEMA/DMA hydrogel in 0.0018 $MNaN_3$ (65%*T*, 0.8%*C*, 10%DMA). The observations based on Figures 4 and 5 are the same. The best way to predict size-exclusion effects for a particular solute in a particular gel is to know the pore-size distribution. We illustrate this by showing results from calculations by Walther et al. using the pore-size distributions that they obtained in Figures 4 and 5. These calculations, described in detail in Refs. 11 and 20, do indeed better approximate the experimental data than does the fiber or pore model.

Returning to Table I, we observe that the calculated pore sizes are larger than the fitted pore sizes for the poly-NIPA gels and vice versa for the poly-HEMA/DMA gels. The mean pore sizes determined by Walther et al. are always smaller than those obtained by fitting the SUP model to the data. Presumably, the fitted pore sizes are larger than the experimentally derived mean pore size because the fitted pore size must compensate for the true distribution of sizes with a single parameter; that this can be done well is remarkable. For a given pair of gels of the same composition but different volume fractions, the ratio of the fitted pore sizes is the same as the ratio of mean pore sizes reported by Walther et al. The ratio of the fitted pore size to the mean

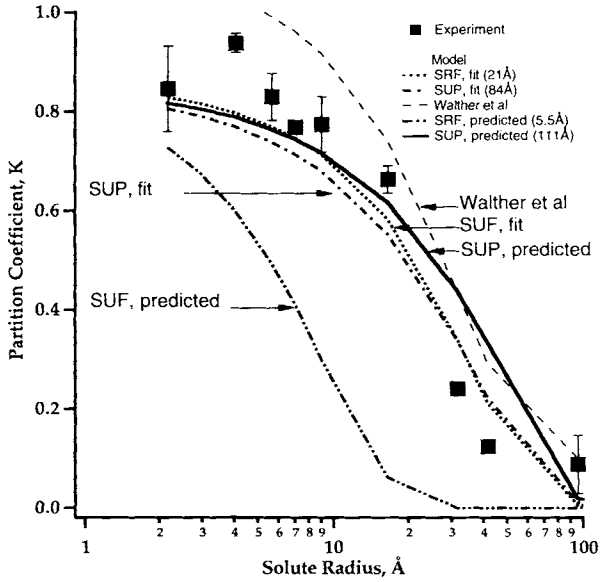

Figure 4 Effect of solute radius on partition coefficient for partitioning of PEG and PEO into poly-NIPA hydrogels (15%*T*, 1%*C*) in water at 32°C. Experimental data are shown by filled squares. Calculations by Walther et al. agree best with experiment. Calculations using Schnitzer's fiber and pore models with adjusted and a priori parameters are shown for comparison. The fiber and pore models, when fit to experiment, predict essentially the same size-exclusion curve. Of the a priori calculations, the pore model agrees best with experimental data. The fit value of the fiber radius is 21 Å; the estimated value is 5.5 Å. The fit value of the pore radius is 84 Å; the estimated value is 111 Å.

pore size is nearly constant for the poly-NIPA gels (3.0) and for the poly-HEMA/DMA gels (2.0) with the exception of the data for the 65%*T* 0.2% 10%DMA poly-HEMA/DMA gels. Further, it is tempting to conclude from the data for the poly-NIPA gels that the mean pore size is inversely related to the volume fraction of the polymer; the volume fraction of the polymer at 32°C is 1.9 times the volume fraction at 25°C, and the mean pore size at 25°C is 1.9 times the mean pore size at 32°C. Unfortunately, this relationship is not borne out nearly as well by the data for the poly-HEMA/DMA gels.

CONCLUSIONS

This work discusses how to predict or correlate size-exclusion effects in hydrogels. Calculated results are compared to experimental partitioning data in poly-NIPA and poly-HEMA/DMA hydrogels. A quantitative understanding of size-exclusion effects is necessary as a starting point for the prediction of partition coefficients for solutes whose interactions with hydrogels go beyond free-volume effects. The best quantitative understanding is provided by experimental pore-size distribution data for the material; such data provide the well-known universal calibration curves in size-exclusion gel chromatography. Once obtained, the experimental size-exclusion curve can be correlated almost equally well by an appropriate pore or fiber-matrix model. However, the necessary experimental effort is large, perhaps prohibitively large. An a priori calculation would save much time and effort.

The distribution coefficient derived for the random-cylindrical-pore model by Schnitzer (SRP model) is incorrect in the limit where the solute radius approaches the pore radius. When fit to experimental data, differences between cylindrical-fiber-matrix models (LKF and SRF) and cylindrical-pore models (SUP and DP) are greatest for partition coefficients near zero or unity. Models accounting for the flexibility of polymeric solutes are most relevant for polymeric solutes whose radius of gyration is on the order of or greater than the mean pore size. The effects of solute concentration are insignificant at solute volume fractions of 1% as used in size-exclusion experiments by Walther et al.[22,25]

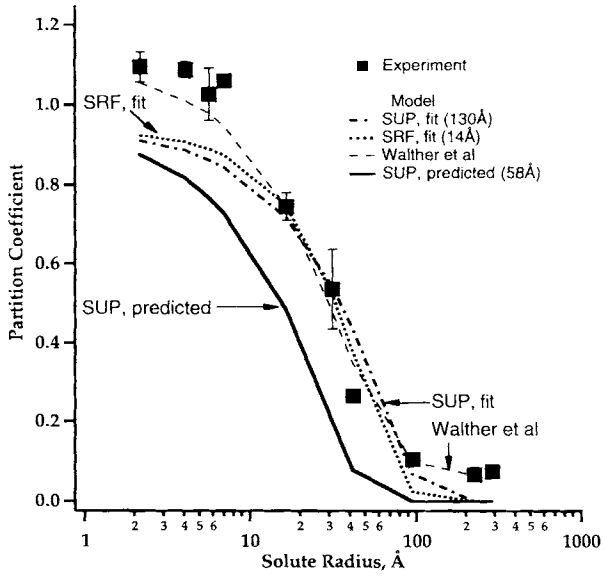

Figure 5 Effect of solute radius on partition coefficient for partitioning of PEG and PEO into poly-HEMA/DMA hydrogels (65%*T*, 0.8%*C*, 10%DMA) in 0.0018*M* aqueous sodium azide at 25°C. Experimental data are shown by filled squares. Calculations by Walther et al. agree best with experiment. For comparison, calculated results are shown for Schnitzer's pore and fiber models with fit parameters and for Schnitzer's pore model with an estimated pore size.

For the design of novel gels, it is desirable to predict the size-exclusion curves, especially as a function of polymer volume fraction, $\%T$, and $\%C$. Such predictions provide guidance for the synthesis of a gel for a particular application where the permeation of a specific solute is important. At present, it is not possible to do this quantitatively, but calculations using Schnitzer's uniform-cylindrical-pore model (SUP) appear to provide the best a priori estimate for the effects of polymer volume fraction. In the data examined here, the volume fraction of polymer constituting the network was not greater than 15% at equilibrium, and the polymeric solutes were sufficiently flexible and dilute to permit neglect of the corrections of Davidson et al.[12] and Fanti and Glandt.[23]

The SUP model requires knowledge of the polymer volume fraction (or swelling capacity), solute radius, and pore radius at conditions where we wish to know the size-exclusion curve. The pore radius can be estimated by using the nominal crosslink density and light-scattering data for the conformation of the polymer. The effect of $\%T$ on the topographical crosslink density enters in the calculation of the size-exclusion curve only through its effect on the polymer volume fraction because we assume that entanglements are quite loose. The effect of $\%T$ and $\%C$ could perhaps be better taken into account by calculating an effective crosslink density using stress–strain measurements, but our attempts to do so were not successful. Predicting the effects of $\%T$ and $\%C$ on size-exclusion curves remains an area for continuing research.

This work was supported by the Director, Office of Energy Research, Office of Basic Energy Sciences, Chemical Sciences Division of the U.S. Department of Energy under Contract No. DE-AC03-76SF00098 and by the National Institutes of Health. The authors are grateful to John Baker, Brooks Boyd, Michael Kremer, Ronald Siegel, and Dieter Walther for helpful discussions. A.P.S. is grateful to the National Science Foundation for a fellowship.

NOMENCLATURE

Roman

Å	angstrom (10^{-10} m)
B_n	roots of the Bessel function J_0
$\%C$	percent crosslinking monomer (on a diluent free basis)
D_0	diffusion coefficient of solute at infinite dilution ($m^2\ s^{-1}$)
k_b	Boltzmann's constant ($J\ K^{-1}$)
J_0	Bessel function of the first kind of order zero
K	partition coefficient
l	step length of polymer chain (m)
L	length of fibers per unit volume ($L = (1/V)\ \sum_i n_i L_i$) ($m^{-2}$)
L_i	length of an individual fiber
$\bar{M}_c$	average molecular weight between crosslinks ($g\ mol^{-1}$)
MW	molecular weight ($g\ mol^{-1}$)
n_i	number of fibers of length L_i
N	number of monomers in the chain
r_f	fiber radius (m)
r_p	pore radius (m)
r_s	solute radius (m)
$\langle r^2_{e-e} \rangle$	mean square end-to-end distance (m^2)
$\langle s^2 \rangle$	mean square radius of gyration (m^2)
T	temperature (K)
$\%T$	ratio of monomer to diluent at synthesis ($g\ mL^{-1}$)
V	volume (m^3)
X	$= \%C/(100 - \%C)$

Greek

β	ratio of solute radius to pore radius
ν_c^0	volume of pore space per unit volume (porosity)
ν_e^0	volume fraction excluded to a point solute
ϕ_p	polymer volume fraction
η_0	viscosity of solvent ($kg\ m^{-1}\ s^{-1}$)
λ_G	ratio of radius of gyration to pore radius ($\lambda_G = \sqrt{\langle s^2 \rangle}/r_p$)
ξ	mesh size of polymer network (m)
τ	dimensionless reduced temperature [$\tau = (T - \theta)/\theta$]
θ	temperature where second osmotic virial coefficient for polymer becomes zero (K)

REFERENCES

1. S. Hussain, M. S. Mehta, J. I. Kaplan, and P. L. Dubin, *Anal. Chem.*, **63**, 1132 (1991).
2. N. A. Peppas, H. J. Moynihan, and L. M. Lucht, *J. Biomed. Mater. Res.*, **19**, 397 (1985).
3. A. G. Ogston, *Trans. Faraday Soc.*, **54**, 1754 (1958).
4. T. C. Laurent and J. Killander, *J. Chromatogr.*, **14**, 317 (1964).
5. J. Schnitzer, *Biophys. J.*, **54**, 1065 (1988).

6. J. C. Giddings, E. Kucera, C. P. Russell, and M. N. Myers, *J. Phys. Chem.*, **72,** 4397 (1968).
7. H. Yasuda, C. E. Lamaze, and L. D. Ikenberry, *Makromol. Chem.*, **19,** 118 (1968).
8. N. A. Peppas and C. T. Reinhart, *J. Membr. Sci.*, **15,** 275 (1983).
9. E. F. Casassa, *J. Polym. Sci. Part B,* **5,** 773 (1967).
10. E. F. Casassa, *Separat. Sci.*, **6,** 305 (1971).
11. E. F. Casassa, *J. Phys. Chem.*, **75,** 3929 (1971).
12. M. G. Davidson, U. W. Suter, and W. M. Deen, *Macromolecules,* **20,** 1141 (1987).
13. D. H. Walther, H. W. Blanch, and J. M. Prausnitz, LBL Report #LBL-34875, Lawrence Berkeley Laboratory, 1993.
14. K. Kubota, S. Fujishige, and I. Ando, *J. Phys. Chem.*, **94,** 5154 (1990).
15. R. F. S. Freitas, PhD Thesis, University of Minnesota, 1986.
16. J. P. Baker, L. H. Hong, H. W. Blanch, and J. M. Prausnitz, *Macromolecules,* **27,** 1446 (1994).
17. M. M. Prange, H. H. Hooper, and J. M. Prausnitz, *AIChE J.*, **35,** 803 (1989).
18. J. P. Baker, PhD Thesis, University of California/Berkeley, 1993.
19. T. Canal and N. A. Peppas, *J. Biomed. Mater. Res.*, **23,** 1183 (1989).
20. C. Migliaresi, L. Nicodemo, L. Nicolais, and P. Passerini, *J. Biomed. Mater. Res.*, **15,** 307 (1981).
21. J. Janácek and J. Hasa, *Coll. Czech. Chem. Commun.*, **31,** 2186 (1966).
22. D. Walther, G. H. Sin, H. W. Blanch, and J. M. Prausnitz, *Polym. Gels Networks,* to appear.
23. L. A. Fanti and E. Glandt, *AIChE J.*, **35,** 1883 (1989).
24. L. A. Fanti and E. Glandt, *J. Colloid Interfac. Sci.*, **135,** 385 (1990).
25. D. H. Walther, G. H. Sin, H. W. Blanch, and J. M. Prausnitz, *J. Macromol. Sci. Chem. Phys. Rev. Macromol. Chem. Phys.*, **B33,** 277–286 (1994).

Received January 18, 1995
Accepted August 21, 1995